Cure Kinetics, Bonding Performance, Thermal Degradation, and Biocidal Studies of Phenol-Formaldehyde Resins Modified with Crude Bio-oil Prepared from *Ziziphus mauritiana* Endocarps

Shakir Ahmad Shahid,[a] Muhammad Ali,[a] and Zafar Iqbal Zafar [b,*]

Crude bio-oil, extracted from endocarp bio-waste of *Ziziphus mauritiana* by direct liquefaction (ethanol-water 1:1 w/w; 300 °C), was used to replace petro-phenol (30% to 75% w/w) in the development of bio-oil-phenol formaldehyde (BPF) resol resins. Cure kinetics of the BPF resins were studied by the DSC method, while the thermal degradation was studied by the TGA method. Bonding performance of the BPF resins was measured by single lap-shear method, while biocidal properties were investigated by antifungal index (%) and termite mortality (%) test. The DSC studies revealed that beyond 45% bio-oil incorporation (BOI), the curing process of the BPF resins got deferred. The TGA studies showed that BOI decreased the thermal stability of the BPF resins by lowering the decomposition temperatures and the char residue. The measured values of antifungal index (%) and termite mortality (%) revealed that incorporation of bio-oil enhanced the fungal and termite resistance of the resins. From data of thermal cure, bonding strength, thermal stability, and biocidal properties of the BPF resins it appears that petro-phenol could be substituted by up to 45% w/w of crude bio-oil safely in the development of bio-oil-phenol formaldehyde resol resins.

Keywords: Crude bio-oil; Bio-wastes; Ziziphus mauritiana; Bio-oil phenol formaldehyde resins; Differential scanning calorimetry; Bonding strength; Thermogravimetry; Termite resistance test

Contact information: a: Department of Chemistry, University of Sargodha, Sargodha-40100, Pakistan; b: Institute of Chemical Sciences, Bahauddin Zakariya University, Multan-60800, Pakistan;
** Corresponding author: drzafarbzu@hotmail.com*

INTRODUCTION

Worldwide there are growing concerns about the sustainability of economic growth due to the ever-increasing consumption of natural resources. Undoubtedly the development of synthetic materials has managed to bridge the gap between demand and supply; however the production of such materials has posed environmental issues of toxicity and non-biodegradability. Hence, during the past few decades, the security of the environment and the sustainability of technological processes have emerged as major driving forces motivating the development of eco-friendly materials through utilization of renewable resources.

Amongst various possible renewable resources, ligno-cellulosic biomass holds an immense potential. Drupe endocarp biomass, which is a major agricultural and forest bio-waste product, is found all over the world. Generally the drupe endocarp consists of 42% wt. lignin, 30% wt. cellulose, and 1.5% wt. ash (Dardick *et al.* 2010; Mendu *et al.* 2011). In 2004, the total global estimated yield of the endocarp was 2.4×10^7 tons, with high

production density in South Asia, including Pakistan (Mendu *et al.* 2012). *Ziziphus mauritiana,* locally known as "bair" or "beer", is a fruit plant abundantly found throughout Pakistan. The endocarp stone of this fruit, which is normally discarded as a waste, can be utilized for production of a variety of useful bio-materials.

Phenol formaldehyde (PF) resin is the most widely used wood-based thermosetting binder due to its excellent durability, thermal stability, and low formaldehyde emissions (Lee and Oh 2010). Phenol, which is the basic raw material used in synthesis of PF resin, is a petro-chemical, and thus is subject to ever rising prices and frequent supply fluctuations. Hence considerable research has been conducted to explore different bio-materials as petro-phenol substitutes to address the supply and price issues (Wang *et al.* 2009a,b; Zhang *et al.* 2013). In this regard, substitution of phenol by bio-oil for development of bio-oil based PF resins has been the subject of many studies (Amen-Chen *et al.* 2002; Alma and Basturk 2006; Cheng *et al.* 2011; Shahid *et al.* 2014).

Wood, which is a wonderful gift of nature to mankind, finds its extensive usage in a number of applications, especially in the fuel and construction sectors. However, due to rapid deforestation and increased global warming, the development of wood composite materials by efficient production methods offers a sustainable solution to lessen the burden on conventional wood. The wood composites have many advantages over natural wood with respect to uniformity, light weightiness, and high stiffness. However, like natural wood, these composites are susceptible to a number of deteriorating agents such as fire, fungus, and the termites.

Termites, which are one of the most destructive bio-degradation agents, are widely spread throughout the world. Termites are a major cause of wood deterioration in many parts of the world including the southern United States and Hawaii (Lee *et al.* 2004; Istek *et al.* 2005; Verma *et al.* 2010), with an estimated annual damage of about U.S. $50 billion worldwide annually (Korb 2007). A number of techniques have been employed to counter the termite attack; however a simple solution to reduce the termite damage is by employing the termite-resistant materials derived from wood resources. It has been reported that extractives of a few wood species possess a significant resistance against termite attack (Behr 1972; Grace and Yamamoto 1994). Amongst various bio-materials, the bio-oils possess insecticidal properties (Burt 2004) and have been actively investigated as protection measure against wood deterioration (Mourant *et al.* 2005; Mourant *et al.* 2007; Temiz *et al.* 2010, 2013).

This study is a continuation of investigations for developing a suitable synthesis of bio-oil-phenol formaldehyde (BPF) resins by utilizing locally available bio-waste resources with the broad objective of producing eco-friendly sustainable materials. The present work is conducted to evaluate the effects of bio-oil incorporation (BOI) on cure kinetics, thermal degradation, and biocidal properties of the BPF resins, along with the optimization of BOI levels in the PF resin.

EXPERIMENTAL

Materials

The ACS reagent-grade chemicals (ethanol, acetone, and ethyl acetate) supplied by Sigma-Aldrich (St. Louis, MO) were used as received. Commercial-grade phenol of 99% purity, formaldehyde solution (35 wt.% aqueous solution), and sodium hydroxide

(40 wt.% aqueous solution) were used. The waste endocarp bio-waste of *Ziziphus mauritiana* was collected from a rural location in the Jhang district of Pakistan.

Methods

Preparation of crude bio-oil from endocarp bio-mass of Ziziphus mauritiana by direct solvolytic liquefaction method

The details of bio-oil the preparation procedure from endocarp shells of *Ziziphus mauritiana* are given in a previous article (Shahid *et al.* 2014). In brief, 50 g biomass powder (20 mesh-Tyler standard) and 500 g (ethanol-water; 1:1 w/w) co-solvent mixture were charged into a 1000-mL Parr high-pressure steel autoclave reactor. The reactor was pressurized to 2.0 MPa with nitrogen, and then the temperature was raised to 300 °C at a steady rate of 10 °C/min and kept at 300 °C for 15 min before it was cooled. After venting the gaseous products, the processed biomass was rinsed with acetone, and the liquid products were filtered from the solid residue. After evaporating the ethanol and acetone, the remaining liquid solution was extracted with ethyl acetate. Crude bio-oil was produced by evaporating the ethyl acetate solvent under reduced pressure.

Synthesis of conventional PF and bio-oil-phenol formaldehyde resins

The phenol-formaldehyde resol resins were synthesized according to a procedure reported in a previous article (Shahid *et al.* 2014). In brief, a three-necked 100-mL flask equipped with a magnetic stirrer and cooling unit was used as the reaction vessel. Phenol and formaldehyde were used at a molar ratio of 1:2, while NaOH was used as catalyst at 0.1:1 molar ratio of NaOH/phenol. The conventional PF (CPF) resin was prepared by charging the calculated amounts of phenol, ethanol, sodium hydroxide solution (50 wt. %), and water (to make up 45% solids) into the reaction flask. The reaction medium was heated to 80 °C and then maintained at this temperature for 1 h with continuous stirring. Then the calculated amount of formaldehyde was added drop-wise while maintaining the reaction medium at 80 °C for 3 h, before stopping the reaction by rapid cooling. Ethanol was evaporated at 60 °C under reduced pressure to produce a viscous resin solution. The BPF resins were developed by substituting the petro-phenol with equivalent amount of bio-oil at 30, 45, 60, and 75 wt.%, and were coded as BPF30, BPF45, BPF60, and BPF75, respectively. The resin solution was neutralized by aminosulfonic acid to a pH 6.5 and then air-dried to a solid powdered form.

Characterization of the synthesized resin samples

The thermal cure kinetics of the resin samples were studied by the dynamic differential scanning calorimetry (DSC) method (DSC 1, Mettler-Toledo, Switzerland) at different heating rates (5, 10, 15, and 20 °C/min) under a 50 mL/min N_2 flow, as reported by earlier studies (Wang *et al.* 2009a; Cheng *et al.* 2011). Multiple heating rates were used to avoid the possible inconsistency in results due to use of a single heating rate (Park *et al.* 1999; Vázquez *et al.* 2002). The n^{th} order reaction model (without consideration of the cure reaction mechanism) was applied on results of dynamic DSC study of the resins (Alonso *et al.* 2004) for deriving relevant kinetic parameters. To calculate the cure kinetic parameters, the Kissinger and Crane equations (Kissinger 1957; Crane *et al.* 1973) were applied:

$$\text{Kissinger Equation: } d\ln(\beta/T_p^2)/d\ln(1/T_p) = -E/R \quad (1)$$

Crane Equation: $d \ln\beta/d(1/T_p) = -E/(nR)$ (2)

In these equations T_p (K) is the peak temperature in DSC thermograms, β is the heating rate, n is the order of cure reaction, E (kJ/mol) is the apparent activation energy, and R (8.314 J mol^{-1} K^{-1}) is the universal gas constant. The apparent activation energy (E) and the reaction order (n) were calculated from plots of $\ln(\beta/T_p^2)$ versus $1/T_p$, and $\ln\beta$ versus $1/T_p$, respectively.

The adhesive strength of the resins for wood-to-wood system was measured by a single lap-shear method according to the procedure reported by Wang *et al.* (1995), with some modifications. In summary, 1.27 cm wide, 0.162 cm thick, and 10.61 cm long flakes were cut from a wood block of white pine (*Pinus* spp.) having grain direction parallel to the length so as to ensure complete failure. After cutting, one side of the flakes was made smooth and then placed between glass plates while conditioning at room temperature (25 °C) and a relative humidity (RH) of 65 ± 5% until constant weight was reached. Approximately 20 mg (±2 mg) of adhesive resin was applied on the smooth surface side of the flakes to give a thin, uniform, and continuous adhesive film. The area of overlap for the flakes was 1.27 cm wide × 2.54 cm long. After an open assembly time of 20 min, the two flakes were then lapped over the length of their coated ends, and a lap shear joint was manufactured by hot-pressing at a temperature of 150 °C and a pressure of 10 N/mm^2 for 5 min. After bonding, the flakes were again conditioned at 25 °C and 65 ± 5% RH until constant weight before testing. The tensile lap-shear bond strength tests were conducted on an Instron Universal Testing Machine Model 4204 (Canton, MS) at a crosshead speed of 10 mm/min. The maximum loads taken by the samples were recorded and average shear strength of five test specimens was determined. The tensile shear strength of the resins under wet conditions was measured by first soaking the specimens in neutral water (pH~7) for 2 h, and then drying at room temperature to constant weight.

The resins were cured by heating the resin sample at 100 °C for 1 h, at 150 °C for 2 h, and then finally at 180 °C for 2 h. Thermal stability of the cured resin sample was examined by using thermogravimetric analysis (TGA) (TGA 1000i, Instrument Specialists Inc., USA) at a heating rate of 10 °C/min under 20 mL/min N_2 flow at the temperature range of 25 °C to 700 °C.

The termicidal properties of the resins were measured by the procedure reported by Grace *et al.* (1992), with some modifications. The resin solution was diluted with distilled water to 10% (w/w) concentration. Two filter papers (Whatman No. 2) were saturated with the diluted resin solution and then air dried. The treated papers were moistened with 4 mL distilled water and then placed in a glass jar with mesh lid. A plastic beaker containing soaked cotton wool was inverted on the mesh to provide a water source for the insects. Fifty (50) acclimatized (for 24 h) worker termites (*Heterotermes indicola*) were introduced in each jar placed in an unlighted area with alternate day check for the mortality rate. Three trials were performed for each type of resin sample.

The fungicidal properties of the resins were studied by performing antifungal assays according to procedure reported by Rivilli *et al.* (2011), with some modifications. Two typical wood decay fungi, one white-rot fungi (*Trametes versicolor*), and one brown-rot fungi (*Gloeophyllum trabeum*) were used as test strains. The fungal strains were obtained from First Fungal Culture Bank of Pakistan (FCBP), Institute of Agricultural Sciences (IAGS), Punjab University, Lahore. In brief the resin solution was diluted with distilled water to 10% (w/w) concentration. Agar potato glucose (APG)-resin mixture was prepared in 4:1 (v/v) ratio. The sterilized Petri dishes having sterile

APG-resin mixture were inoculated by transferring the mycelium. The inoculated plates were incubated at 37 °C till the mycelium of fungi reached the edges of the control plate having just Agar potato glucose (APG). At the end of the incubation period, the growth inhibition was observed and antifungal index was calculated with reference to the control sample according to formula: antifungal index (%) = (1 - D_a/D_b) × 100 where D_a is the diameter of the growth zone in the experimental plate and D_b is the diameter of the control plate.

RESULTS AND DISCUSSION

Thermal Cure Kinetics of the Synthesized Resins

The DSC thermograms of the resins are exhibited in Fig. 1, while T_p, ΔH_0, and α_p of the resin cure at heating rate of 10 °C/min are presented in Table 1.

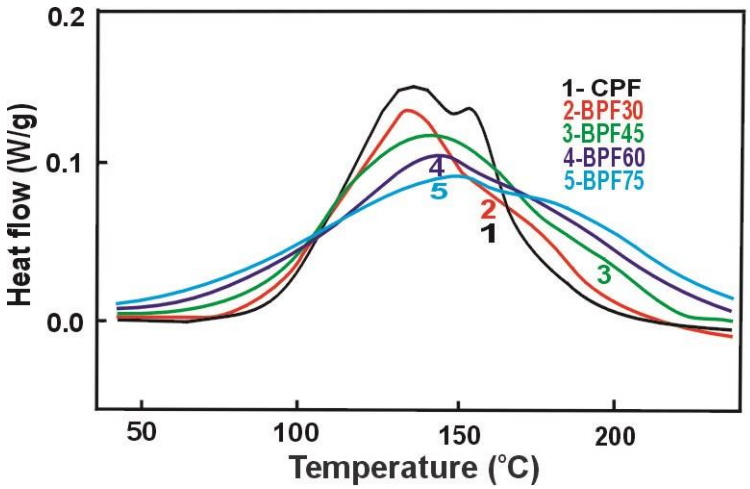

Fig. 1. DSC thermograms of the resins with different BOI% at heating rate of 10 °C/min

Table 1. The Peak Temperature, Reaction Heat, and Conversion Rate of the Resins at Peak Temperature at Heating Rate of 10 °C/min

Resin code	BOI (%)	T_p (°C)	ΔH_0 (J.g^{-1})	α_p
CPF	0	139.3	297.5	0.51
BPF30	30	136.3	313.9	0.53
BPF45	45	139.2	299.7	0.48
BPF60	60	144.3	261.4	0.45
BPF75	75	150.8	239.8	0.41
T_p= Peak Temperature; ΔH_0 = total reaction heat; α_p =conversion at peak temperature				

Table 1 indicates that total reaction heat (ΔH_0) of the resin cure initially increased with the incorporation of bio-oil; however once the BOI % exceeded a certain level (*ca.* 45 wt.%) the ΔH_0 started decreasing. A similar pattern of initial increase and then decrease in α_p of the resin cure reaction was observed with gradual increase of BOI % level in the resin formula. The general decreasing trend in values of ΔH_0 may be attributed to increase in molecular weights (M_w) of the BPF resins (Shahid *et al.* 2014), as it is generally believed that less crosslinking is needed for relatively high molecular weight resins and consequently less reaction heat is evolved. However, the increase in

value of ΔH_0, when BOI% ≤ 45wt. %, may be attributed to role of bio-oil as an efficient crosslinking agent (Shahid *et al.* 2014). Figure 1 also demonstrates that with the increase of BOI%, the main exothermic peak of the cure reaction gradually widened. The findings are generally consistent with the reports of similar earlier studies (Wang *et al.* 2009a; Cheng *et al.* 2011, 2012).

The main exothermic peak observed in Fig. 1 is probably due to inter-condensation of methylol groups, as well as crosslinking of methylol groups with phenolic moieties present in the bio-oil to form methylene and ether bridges, as attributed in earlier studies (Gabilondo *et al.* 2007; Wang *et al.* 2009a; Cheng *et al.* 2011, 2012). The shoulder peaks may be attributed to addition reactions of free monomers and conversion reactions of ether bridges to methylene bridges, as cited by some other studies (Wang *et al.* 2009a; Cheng *et al.* 2011; 2012). As stated by Wang *et al.* (2005) the onset/peak/end temperatures of the thermal cure of the resol resins may be regarded as gel temperature, curing temperature, and postcure temperature, respectively.

The measured values of T_p of the resins at multiple heating rates (5, 10, 15, and 20 °C/min) are presented in Table 2. The T_p values at heating rate of 5 °C/min ranged from 131.3 to 145.9 °C, while at heating rate of 10 °C/min the T_p values ranged from 136.4 to 150.8 °C. The T_p values at heating rate of 15 °C/min ranged from 142.4 to 156.1 °C, while at heating rate of 20 °C/min the T_p values ranged from 148.7 to 160.5 °C. The T_p values at heating rate of 0 °C/min obtained by linear extrapolation ranged from 125.2 to 141.0 °C.

Table 2. DSC Peak Cure Temperatures (T_p) of the Resins at Multiple Heating Rates

Resin code	BOI (%)	T_p (°C) at multiple heating rates (β) (°C/min)			
		5	10	15	20
CPF	0	134.2	139.3	144.7	150.8
BPF30	30	131.4	136.3	142.5	148.6
BPF45	45	134.3	139.2	144.7	150.6
BPF60	60	139.4	144.3	149.9	155.1
BPF75	75	145.9	150.8	156.1	160.5

The plots of DSC kinetic analysis by the Kissinger equation are displayed in Fig. 2a, and the plots of DSC kinetic analysis by the Crane equation are displayed in Fig. 2b.

The calculated values of energy of activation (E) and order of the cure reaction (n^c) for all the resins are exhibited in Table 3, which were calculated from plots of DSC kinetic analysis by Kissinger and the plots of DSC kinetic analysis by Crane equation. The E values of all the resins ranged from 104 to 134 (kJ/mol), while the n^c values of all the resins ranged from 0.938 to 0.950. The table shows the effect of bio-oil incorporation on the dynamic DSC profiles of the resins. The results indicate that curing temperatures of the resins initially decreased with the incorporation of bio-oil; however once the BOI % exceeded a certain level (*ca.* 45 wt.%) the curing temperature of the resins started increasing. A similar pattern of initial decrease and then increase in E of the resin cure reaction was observed with gradual increase of BOI % level in the resin formula. The calculated results for E and n^c are similar to the results cited by some earlier studies (Wang *et al.* 2009a; Cheng *et al.* 2011; Cheng *et al.* 2012).

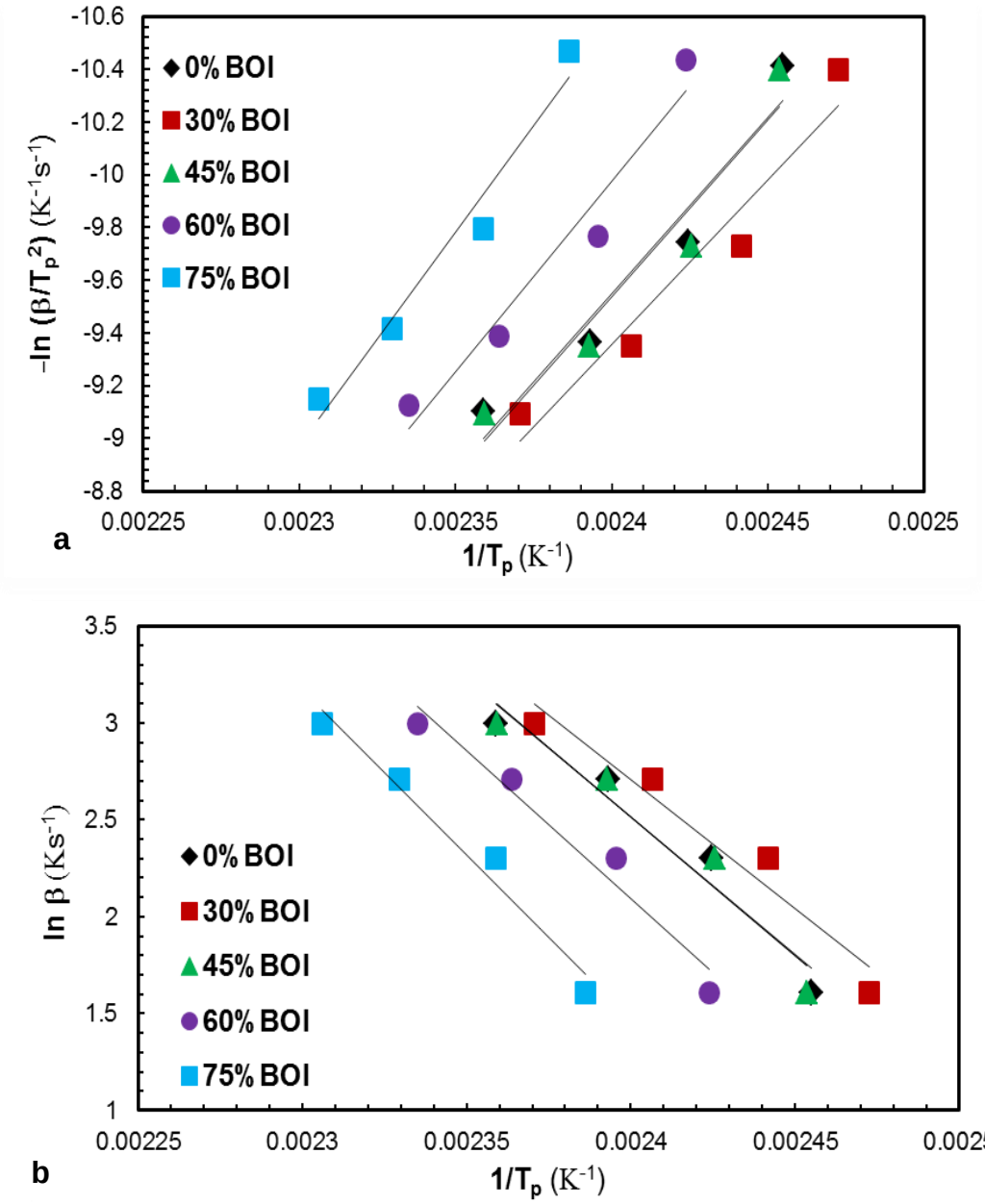

Fig. 2. (a) Plots of DSC kinetic analysis by Kissinger equation and (b) plots of DSC kinetic analysis by Crane equation

Table 3. Energy of Activation (*E*) and Order of Cure Reaction (n^c) Calculated from Kissinger and Crane Equations for the Resins

Resin code	BOI (%)	Slope of Kissinger Equation =-*E*/*R*	*E* (kJ/mol)[b]	Slope of Crane Equation =-*E*/ (*nR*)	n^c
CPF	0	-13356.22	111	-14187.37	0.941
BPF30	30	-12514.86	104	-13340.97	0.938
BPF45	45	-13552.49	113	-14383.53	0.942
BPF60	60	-14436.07	120	-15276.67	0.945
BPF75	75	-16106.60	134	-16959.07	0.950
[b]based on the Kissinger equation; [c]based on the Crane equation					

As the energy of activation of the cure reaction and the peak temperature of the cure thermograms are directly related with each other, both may be explained on the same grounds. The initial decrease in peak cure temperatures (T_p) and subsequent energy of activation (E) of the resin cure reactions, on incorporation of bio-oil, may be attributed to increase in molecular weights (M_w) of the BPF resins (Shahid *et al.* 2014). It is generally believed that lower activation energy is needed for high M_w resins to cure (Park *et al.* 1998; Anwar *et al.* 2009; Wahab *et al.* 2012), meaning thereby that high M_w resins would cure at low temperatures. The initial decrease in curing temperature and the E may be also be attributed to promotional catalytic effect of lingo-cellulosic derivatives present in the bio-oil on the cure reaction, as reported by some other studies (Vázquez *et al.* 2002; Turunen *et al.* 2003; Khan *et al.* 2004; Lei and Wu 2006; Wang *et al.* 2009a; Hu *et al.* 2013). The role of bio-oil as an efficient crosslinking agent due to presence of multiple reactive sites (Hu *et al.* 2013) may also be taken as a reason for such decrease in T_p and E of the curing reaction.

The increase in E and cure temperature of the BPF resins, when BOI% exceeded the limit of *ca.* 45 wt.%, is contrary to the general principal of low E and low cure temperatures for high M_w resins. This increase in E and T_p of cure reactions of the resins, when BOI% exceeded the limit of *ca.* 45wt.%, may be attributed to relative less reactivity of the bio-oil as compared to the petro-phenol (Lee *et al.* 2000; Wen *et al.* 2013). It may be presumed that during the resin synthesis stage the factor of relative less reactivity of the bio-oil translated itself into production of BPF resins having lower density of potential polymerization points, which are required for crosslinking during cure reactions, as explained in detail in previous work (Shahid *et al.* 2014). Beyond 45% BOI level the decline in density of polymerization points on the synthesized BPF resins became significant enough, and thus to compensate the decreasing polymerization reactivity of the BPF resins the E and T_p of the cure reactions started increasing. Hence it may be assumed that when BOI% exceeded the limit of *ca.* 45wt.%, the increase in E and T_p due to relative less bio-oil reactivity over-rode the decrease in E and T_p of the cure reaction due to increase in M_w of the resins, and thus resulted in net increase in E and T_p of the cure reaction.

In dynamic DSC thermograms, as illustrated in Table 2, it is generally observed that on increasing the heating rate, the exothermic peaks gradually drift toward the higher temperature side, which means that the condensation reaction shifted toward higher temperatures with the increase of heating rates. It also appeared that with the increase of heating rate the frequency of high temperature shoulder peaks, which are probably due to conversion of ether bridges into methylene bridges, became more conspicuous. The increased frequency of shoulder peaks may be attributed to an increased rate of the conversion reaction of ether bridges into methylene bridges with the increase of rate of heating.

The DSC results displayed in Fig. 1, Table 1, Table 2, and Table 3 suggest that incorporation of bio-oil in the resin could play two opposite roles, depending on the BOI% level, during the curing reaction. At low BOI levels (BOI% < *ca*. 45wt. % *e.g.* BPF30, BPF45), the bio-oil would favor the curing reactions by lowering the E and curing temperatures, while at high BOI levels (BOI% > *ca*. 45wt. % *e.g.* BPF60, BPF75), the bio-oil would exert a retarding effect on the curing reaction by elevating the E and curing temperatures.

From the calculated results of thermal cure kinetics as displayed in Table 3 the order of cure reactions for all the resins is first order (n=0.94-0.95), which is consistent

with the results reported by earlier studies (Wang *et al.* 2009a; Cheng *et al.* 2011; 2012). This suggests that Friedel-Crafts reaction mechanism for condensation reactions occurring during the cure process of all the resins is same. This also suggests that the reaction mechanism for inter-crosslinking of methylol groups, and between methylol and phenolic moieties present in the crude bio-oil is the same. The similar values of E and the order of the reaction (n^c) for the BPF resins to that of the CPF resin suggests that generally similar thermal reactions are going on in cure process for both types of resins, *i.e.*, CPF and BPF resins. The similarity of E and n^c results for CPF and BPF resins also demonstrates the viability of the partial replacement of the petro-phenol with the crude bio-oil.

Bonding Properties of the Synthesized Resins

The measured values of the tensile lap shear strength of the resins at dry and wet conditions are presented in Table 4. The test results of various resin samples indicate that BPF30 resin demonstrated optimal dry bonding strength, while the BPF45 resin displayed the optimal wet bonding strength. Bonding strength of both the BPF30 and BPF45 resins is comparable to the bonding strength of CPF resin.

Table 4. Dry and Wet Tensile Shear Strength Values of the Resins

Resin code	BOI (%)	Shear strength (MPa)	Wet shear strength (MPa)
CPF	0	3.19 (±0.01)	2.59 (±0.01)
BPF30	30	3.34 (±0.01)	2.62 (±0.01)
BPF45	45	3.22 (±0.01)	2.64 (±0.01)
BPF60	60	2.82 (±0.01)	1.91 (±0.01)
BPF75	75	2.50 (±0.01)	1.43 (±0.01)
*Each value represents an average of five samples (± SEM)			

From Table 4 it is observed that shear strength of the BPF resins initially increased with the incorporation of bio-oil; however after 45% BOI level, it started decreasing. The increase in shear strength of the BPF resins may be attributed to decrease in gel/cure times of the BPF resins (Shahid *et al.* 2014), affording optimal resin penetration into the wood surface pores, and to increase in molecular weights of the BPF resins, as indicated by earlier studies (Dunky 1997; Shahid *et al.* 2014). The decrease in shear strength of the BPF resins, when BOI level surpassed the limit of *ca.* 45%, may also be attributed to increase in molecular weights of the BPF resins, decrease in resin gel/cure times, and decrease in potential polymerization points on the BPF resins required for crosslinking during cure process (Shahid *et al.* 2014). It is reported that penetration capacity of binder resins is inversely proportional to their molecular weights (Johnson and Kamke 1992; Johnson and Kamke 1994), and generally the resins having M_w>1000Da cannot anchor properly into nano-sized wood cell wall pores due to less effective penetration (Stamm 1964; Robison 1972; Sellers 1994) during hot press application (Laborie 2002; Huang *et al.* 2012).

It has been reported that in addition to providing mechanical strength *via* penetration into cell walls (Furuno *et al.* 2004; Huang *et al.* 2012), the resin fraction penetrating into cell walls also establishes intermolecular couplings with the hydrophilic (-OH) moieties present on cellulose fibers (Huang *et al.* 2012), and thus blocks them from further affiliations. It may be presumed that due to blockage of these hydrophilic (-OH) moieties the lesser amount of water is absorbed by the cell walls impregnated with

the resin, and consequently less rupturing stress is exerted on the bond line holding the wood surfaces together. Hence the initial increase in wet shear strength of the BPF resins may be attributed to cumulative effect of chemical effect of resin fraction penetrating into the cell walls (Huang *et al.* 2012) and to increased dry bonding strength of BPF resin bond line.

Thermal Degradation Properties of the Synthesized Resins

The TG profiles of all the resins are exhibited in Fig. 3, and the measured values of weight loss (WL%) at different temperatures (°C) and char residue at 700 °C of all the resins are presented in Table 5. The T_{p1} (peak temperature of first weight loss event), T_{p2} (peak temperature of second weight loss event), T_{p3} (peak temperature of third weight loss event), and T_{maxd} (temperature of maximum decomposition) are listed in Table 6.

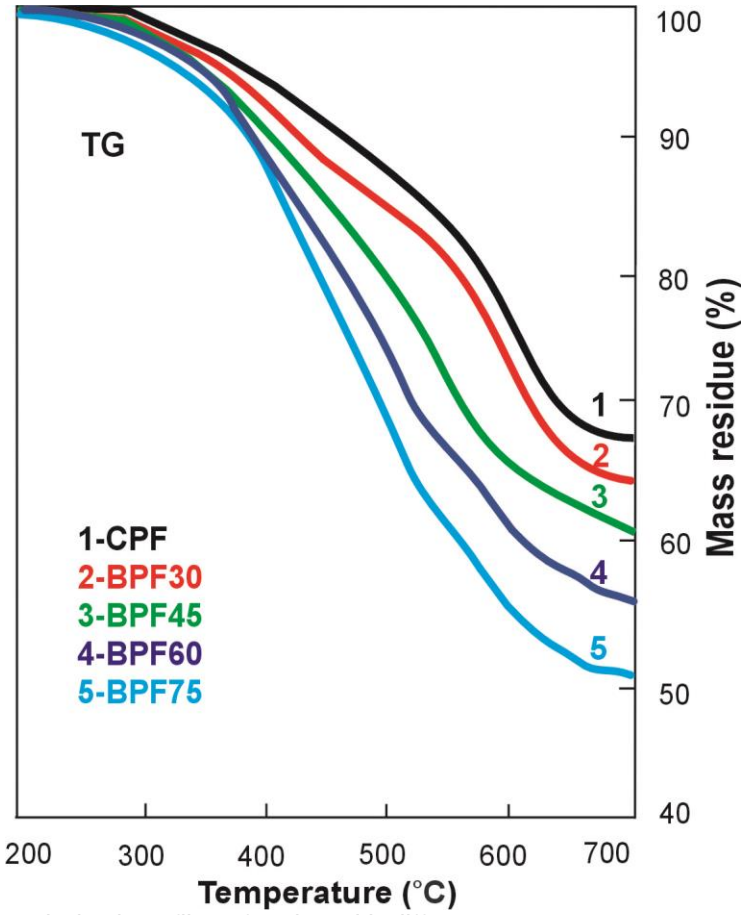

Fig. 3. Thermo-gravimetric (TG) profiles of resins with different BOI%

Table 5. Weight Loss (WL %) Profiles and Char Residue of the Resins at Different Temperatures

Resin code	BOI (%)	Weight loss (WL%) at different temperatures (°C)			Char residue (%) at 700°C
		200 (°C)	400 (°C)	600 (°C)	
CPF	0	0.1	9.9	24.4	67.7
BPF30	30	0.1	12.1	30.1	64.4
BPF45	45	0.3	13.9	32.9	61.0
BPF60	60	0.5	14.8	36.5	56.6
BPF75	75	0.6	17.0	38.9	52.4

Table 6. Peak Temperatures (T_p) of the Different Thermal Events of the Resins

Resin code	BOI (%)	T_{p1} (°C)	T_{p2} (°C)	T_{p3} (°C)	T_{maxd} (°C)
CPF	0	221.7	441.5	587.6	640.6
BPF30	30	225.6	433.6	545.8	571.5
BPF45	45	219.5	399.5	523.4	545.7
BPF60	60	218.8	381.7	517.6	514.7
BPF75	75	212.6	365.5	483.4	488.5

T_{p1} = Peak temperature of first thermal event; T_{p2} = Peak temperature of second thermal event; T_{p3} = Peak temperature of third thermal event; T_{maxd} = Temperature of maximum decomposition

Table 5, Table 6, and Fig. 3, which show the effects of incorporation of bio-oil on thermal profiles of the resin samples, indicate that generally the resin samples exhibited three major decomposition events in temperature zones of 200 to 300 °C, 350 to 500 °C, and 500 to 700 °C, a pattern which is consistent with earlier reports (Kim *et al.* 2004; Chen *et al.* 2008; Wang *et al.* 2009a; Cheng *et al.* 2011; 2012). This pattern may be termed as: postcuring, thermal reforming, and ring stripping (Khan and Ashraf 2007). From thermal profiles of resins it is generally observed that with the increase of BOI% the decomposition zones of the resins drifted toward to the lower temperatures. Similarly the temperature of maximum decomposition (T_{maxd}) and char residue (%) at 700 °C decreased gradually with the gradual increase of BOI% in the resin formula. The initial weight loss of the resins before reaching the temperature limit of 200 °C is generally attributed to removal of water and volatile monomeric units present in the resin samples.

The weight loss during temperature zone of 200 to 300 °C may be attributed to a post-curing reaction of methylol and other functional groups to form methylene bridges (Khan and Ashraf 2007; Chen *et al.* 2008) with release of formaldehyde and water vapors. In this zone additional crosslinking is formed. It is assumed that thermal degradation of cellulosic impurities present in the crude bio-oil and removal of exposed terminal groups also occurs in this temperature zone. During this temperature zone the dimethylene ether bridges also get converted to methylene bridges by breakage and recondensation process, as cited by some similar studies (Vázquez *et al.* 2002; Gabilondo *et al.* 2007; Wang *et al.* 2009a).

The weight loss during the temperature zone of 350 to 500 °C may be attributed to thermal reforming of the cured resin entailing the decomposition of methylene bridges into methyl groups with the formation of phenols and cresols (Chen *et al.* 2008; Khan and Ashraf. 2007). From a careful analysis of TG profiles of resin samples shown in Fig. 3 it appears that temperature zone of 350 to 500 °C is the main weight loss zone for the BPF resins having BOI% more than 45%, which may be attributed to relative easy breakage of potentially unstable bonds like methylene bridges and side chains present on bio-oil molecules as reported by (Wang *et al.* 2009a). In this zone the level of cross-linking is reduced.

The weight loss of the resins while within the temperature zone of 500 to 650 °C may be attributed to ring stripping, entailing the decomposition of backbone phenolic rings (Khan and Ashraf 2007; Chen *et al.* 2008). This may also be attributed to mass loss due to loss of carbon monoxide and methane formed by degradation of methylene bridges (Lee *et al.* 2012). Conley (1965) has reported that phenolic resins are decomposed through oxidation of methylene bridges, regardless of whether resin is exposed to elevated temperatures in air, oxygen, or nitrogen. Through the process of carbonization and graphitization the whole structure of the resin network is collapsed (Costa *et al.*

1997; Chen *et al.* 2008). From TG profiles resin samples shown in Fig. 3 it appears that the temperature zone of 500 to 650 °C is the main weight loss zone for the resins having BOI% equal or lower than 45wt. % which may be attributed to relative stability of the bonds present in resin structure.

As observed from thermal profiles displayed in Table 5, Table 6, and Fig. 3, the gradual drifting of decomposition zones of the resins toward to the lower temperatures that with the increase of BOI% may be attributed to relative easy breakage of breakage of potentially unstable bonds such as methylene bridges and side chains present on bio-oil molecules (Wang *et al.* 2009a). From TG profiles displayed in Fig. 3 it appeared that below 400 °C there was not much difference in thermal stability between CPF and BPF resins; however above 500 °C the BPF resins became significantly inferior than CPF resin, which is evident by the distinctly different values of T_{maxd} (^oC), especially when the BOI exceeded 60%.

From Fig. 3, it appears that generally the rate of mass loss of the resins increased with the increase of temperature up to 600 °C, and then the rate of mass loss started to reach a stable value. The decrease in mass loss rate beyond 600 °C may be attributed to formation of hard coke, which is resistant to degradation. A similar phenomenon of hard coke formation has been reported earlier too (Jae *et al.* 2010). The char layer acts as an insulating barrier to heat transfer for burning materials (Lin *et al.* 2005) and thus decreases the exothermicity of the pyrolysis reaction by limiting the production of combustible gases.

With the increase of BOI% there was a gradual drifting of decomposition zones to the lower temperatures. There was a decrease in T_{maxd} (°C), and a decrease in char residue%, as displayed in Table 5. All these findings indicated that thermal stability of the BPF resins decreased on incorporation of the bio-oil. However, up to 60 wt.% BOI level, the BPF resins exhibited an acceptable level of thermal resistance. For example, the BPF resin having 60% substitution level of phenol demonstrated T_{maxd} higher than 500 °C, and a char residue higher than 55% even at 700 °C. However the decreased thermal stability of the bio-oil based resins may result into low fire performance of the materials manufactured by utilization of such modified resins.

Biocidal Properties of the Synthesized Resins

The measured values of termite mortality (TM%) for the resins at different time intervals are presented in Table 7.

Table 7. Termite Mortality (TM%) for the Resins at Various Time Intervals

Resin code	BOI(%)	TM%/Day			
		1	3	5	7
CPF	0	1.3 (± 0.82)	12.0 (± 1.41)	32.7 (± 2.16)	64.7 (± 2.16)
BPF30	30	4.7 (± 0.82)	16.7 (± 2.94)	44.0 (± 3.74)	70.0 (± 1.41)
BPF45	45	8.0 (± 1.41)	28.7 (± 2.16)	52.7 (± 2.16)	89.3 (± 4.32)
BPF60	60	11.3 (± 2.16)	40.0 (± 1.41)	76.7 (± 2.94)	100 (± 0.00)
BPF75	75	12.7 (± 0.82)	47.3 (± 2.16)	91.3 (± 3.56)	100 (± 0.00)
*Each value represents an average of three samples (± SEM)					

The results exhibited in Table 7 show that mortality (%) of the termites increased with the increase of BOI level in the BPF resins. The BPF60 and BPF75 resins, having 60% and 75% BOI level, exhibited 100% termite mortality on the 7th day of the test

period. The increase in TM% with the increase of BOI % in the resin may be attributed to the termite repellant and insecticidal nature of bio-oil, as reported earlier by some studies (Behr 1972; Burt 2004; Mourant *et al.* 2005; 2007; Temiz *et al.* 2010; 2013). It is reported that the amount of lignin and phenolic contents in a wood determine the termite resistance of wood (Shanbhag and Sundararaj 2013); hence it may be presumed that wood-derived bio-oils having high concentration of lignin and phenolics would exhibit substantial termite repellency. It may also be assumed that termites died due to eating of indigestible lignin derivatives present in bio-oil which caused malfunctioning of their digestive system. As the subterranean termites mainly utilize the cellulose as food source (Bowyer *et al.* 2003), so the BPF resin impregnated filter paper having high concentration of bio-oil may be a less attractive food source for the termites, and they might have died because of starvation. The termite mortality may also be attributed to cannibalistic behavior of termites during food scarcity times, as reported by Nandika (2003). The results of TM% suggest the termite repellent nature of bio-based PF resins.

The values of antifungal index (%) of the resins measured against white-rot fungi (*Trametes versicolor*) and brown-rot fungi (*Gloeophyllum trabeum*) are presented in Table 8.

Table 8. Antifungal Index (%) Values of the Resins for Different Fungal Strains

Resin code	BOI (%)	Antifungal Index (%)	
		Trametes versicolor	*Gloeophyllum trabeum*
CPF	0	30.7 (±1.19)	32.2 (±0.78)
BPF30	30	33.3 (±0.78)	35.5 (±1.39)
BPF45	45	40.4 (±1.19)	41.8 (±1.19)
BPF60	60	42.9 (±0.45)	49.3 (±0.45)
BPF75	75	50.7 (±1.62)	57.8 (±1.56)
*Each value represents an average of three samples (± SEM)			

The results exhibited in Table 8 show that antifungal index (%) of the resins increased with the increase of BOI level in the resin formula. This increase in antifungal index (%) with the increase of BOI % may be attributed to fungicidal nature of the incorporated bio-oil and its constituent molecules, as reported earlier by some studies (Mohan *et al.* 2008; Eller *et al.* 2010; Rivilli *et al.* 2011). Due to environmental constraints attached with chemical based biocides, the termicidal/fungicidal potential of BPF resins is a new avenue promising environment friendly protection regime for the products using BPF resins as binders.

CONCLUSIONS

1. The curing studies conducted by DSC method revealed that beyond a 45% bio-oil incorporation (BOI) level, the curing process of the bio-oil-phenol formaldehyde (BPF) resins became delayed with the increase of energy of activation of the cure reaction.
2. The cure kinetic data demonstrated that all the resins including the conventional phenol formaldehyde (PF) resin cured through a first-order reaction mechanism, indicating the viability of petro-phenol substitution by the crude bio-oil.

3. The thermal degradation studies revealed that thermal stability of the BPF resins decreased with the incorporation of bio-oil. However the thermal stability of the BPF resins was at acceptable levels up to 45wt. % BOI level.
4. The biocidal properties of the BPF resins conducted by termite feeding test and antifungal assays demonstrated that with incorporation of the bio-oil the termicidal and fungicidal capacity of the BPF resins increased.
5. From curing, thermal degradation and biocidal tests it may be concluded that crude bio-oil extracted from endocarp shells of *Ziziphus mauritiana* can be safely incorporated in PF resins at levels up to 45%.

REFERENCES CITED

Alma, M. H., and Basturk, M. A. (2006). "Liquefaction of grapevine cane (*Vitis vinisera* L.) waste and its application to phenol-formaldehyde type adhesive," *Ind. Crops Prod.* 24(2), 171-176. DOI: 10.1016/j.indcrop.2006.03.010

Alonso, M. V., Oliet, M., Pérez, J. M., and Rodríguez, F. (2004). "Determination of curing kinetic parameters of lignin-phenol-formaldehyde resol by several dynamic differential scanning calorimetry methods," *Thermochimica Acta* 419(1-2), 161-167. DOI: 10.1016/j.tca.2004.02.004

Amen-Chen, C., Riedl, B., and Roy, C. (2002). "Softwood bark pyrolysis oil-PF resols. Part 2.Thermal analysis by DSC and TG," *Holzforschung* 56(3), 273-280.

Anwar, U. M. K., Paridah, M. T., Hamdan, H., Sapuan, S. M., and Bakar, E. S. (2009). "Effect of curing time on physical and mechanical properties of phenolic-treated bamboo strips," *Ind. Crops Prod.* 29(1), 214-219. DOI: 10.1016/j.indcrop.2008.05.003

Behr, E. A. (1972). "Decay and termite resistance of medium-density fiberboards made from wood residue," *Forest Prod J*. 22(12), 48-51

Bowyer, J. L., Shmulsky, R., and Haygreen, J. G. (2003). "Forest products and wood science-An introduction," Iowa State University Press, Iowa, USA.

Burt, S. A. (2004). "Essential oils: Their antibacterial properties and potential applications in foods: A Review," *Int. J. Food Microbiol.* 94(1), 223-253. DOI: 10.1016/j.ijfoodmicro.2004.03.022

Chen, Y., Chen, Z., Xiao, S., and Liu. H. (2008). "A novel thermal degradation mechanism of phenol-formaldehyde type resins," *Thermochimica Acta* 476(1), 39-43. DOI: 10.1016/j.tca.2008.04.013

Cheng, S., D'Cruz, I., Yuan, Z., Wang, M., Anderson, M., Leitch, M., and Xu, C. C. (2011). "Use of biocrude derived from woody biomass to substitute phenol at a high-substitution level for the production of biobased phenolic resol resins," *J. Appl. Polym. Sci.* 121(5), 2743-2751. DOI: 10.1002/app.33742

Cheng, S., D'Cruz, I., Yuan, Z., Wang, M., Anderson, M., Leitch, M., and Xu, C. C. (2012). "Synthesis of bio-based phenolic resins/adhesives with methylolated wood derived bio-oil," *J. Appl. Polym. Sci.*126 (S1), E430-E440. DOI: 10.1002/app.35655

Conley, R. T. (1965). "Oxidative degradation of phenol-formaldehyde polycondensation initial degradation reactions," *J. Appl. Polym. Sci.* 9(3), 1117-1126. DOI: 10.1002/app.1965.070090328

Costa, L., Di Montelera, L. R., Camino, G., Weil, E. D., and Pearce, E. M. (1997). "Structure-charring relationship in phenol-formaldehyde type resins," *Polym. Degrad. Stab.* 56(1), 23-35. DOI: 10.1016/S0141-3910(96)00171-1

Crane, L. W., Dynes, P. J., and Kaelble, D. H. (1973). "Analysis of curing kinetics in polymer composites," *J. Polym. Sci.: Polym. Lett. Ed.* 11(8), 533-540. DOI: 10.1002/pol.1973.130110808

Dardick, C., Callahan, A., Chiozzotto, R., Schaffer, R., Piagnani, M. C., and Scorza, R. (2010). "Stone formation in peach fruit exhibits spatial coordination of the lignin and flavonoid pathways and similarity to *Arabidopsis dehiscence*," *BMC Biol.* 8, 1-17. DOI: 10.1186/1741-7007-8-13

Dunky, M. (1997). "Analysis of formaldehyde condensation resins for the wood based panels industry: Status and new challenges," *Proceedings of the Seventh European Panels Products Symposium*, Llandudno, North Wales, UK.

Eller, F. J., Clausen, C. A., Green, F., and Taylor, S. L. (2010). "Critical fluid extraction of *Juniperus virginiana* L. and bioactivity of extracts against subterranean termites and wood-rot fungi," *Ind. Crops Prod.* 32(3), 481-485. DOI: 10.1016/j.indcrop.2010.06.018

Furuno, T., Imamura, Y., and Kajita, H. (2004). "The modification of wood by treatment with low molecular weight phenol-formaldehyde resin: A properties enhancement with neutralized phenolic-resin and resin penetration into wood cell walls," *Wood Sci. Technol.* 37(5), 349-361. DOI: 10.1007/s00226-003-0176-6

Gabilondo, N., López, M., Ramos J. A., Echeverría J. M., and Mondragon I. (2007). "Curing kinetics of amine and sodium hydroxide catalyzed phenol-formaldehyde resins," *J. Therm. Anal. Calorim.* 90(1), 229-236. DOI: 10.1007/s10973-006-7747-3

Grace, J. K., Yamamoto, R. T., and Tamashiro, M. (1992). "Resistance of borate-treated Douglas-fir to the Formosan subterranean termite," *Forest Prod. J.* 42(2), 61-65.

Grace, J. K., and Yamamoto, R, T. (1994). "Natural resistance of Alaska-cedar, redwood, and teak to Formosan subterranean termites," *Forest Prod. J.* 44(3), 41-45.

Hu, X., Wang, Y., Mourant, D., Gunawan, R., Lievens, C., Chaiwat, W., Gholizadeh, M., Wu, L., Li, X., and Li, C. Z. (2013). "Polymerization on heating up of bio-oil: A model compound study," *AIChE J.* 59(3), 888-900. DOI: 10.1002/aic.13857

Huang, Y., Fei, B., Yu, Y., and Zhao, R. (2012). "Effect of modification with phenol formaldehyde resin on the mechanical properties of wood from Chinese Fir," *BioResources* 8(1), 272-282. DOI: 10.15376/biores.8.1.272-282

Istek, A, Sivrikaya, H, Eroglu, H, and Gulsoy, S. K. (2005). "Biodegradation of *Abies bornmülleriana* (Mattf.) and *Fagus orientalis* (L.) by the white rot fungus *Phanerochaete chrysosporium*," *Int. Biodeter. Biodegr.* 55(1), 63-67. DOI: 10.1016/j.ibiod.2004.07.002

Jae, J., Tompsett, G. A., Lin, Y. C., Carlson, T. R., Shen, J., Zhang, T., Yang, B., Wyman, C. E., Conner, W. C., and Huber, G. W. (2010). "Depolymerization of lignocellulosic biomass to fuel precursors: Maximizing carbon efficiency by combining hydrolysis with pyrolysis," *Energ. Env. Sci.* 3(3), 358-365. DOI: 10.1039/b924621p

Johnson, S. E., and Kamke, F. A. (1992). "Quantitative analysis of gross adhesive penetration in wood using fluorescence microscopy," *J. Adhesion*, 40(1), 47-61. DOI: 10.1080/00218469208030470

Johnson, S. E., and Kamke, F. A. (1994). "Characteristics of phenol-formaldehyde adhesive bonds in steam injection pressed flake board," *Wood Fiber Sci.* 26(2), 259-269.

Khan, M. A., and Ashraf, S.M. (2007). "Studies on thermal characterization of lignin substituted phenol formaldehyde resin as wood adhesives," *J. Therm. Anal. Calorim.* 89(3), 993-1000. DOI: 10.1007/s10973-004-6844-4

Khan, M. A., Ashraf, S. M., and Malhotra, V.P. (2004). "Eucalyptus bark lignin substituted phenol formaldehyde adhesives: A study on optimization of reaction parameters and characterization," *J. Appl. Polym. Sci.* 92(6), 3514-3523. DOI: 10.1002/app.20374

Kim, Y. J., Kim, M., Yun, C. H., Chang, J. Y., Park, C. R., and Inagaki, M. (2004). "Comparative study of carbon dioxide and nitrogen atmospheric effects on the chemical structure changes during pyrolysis of phenol formaldehyde spheres," *J. Colloid Interf. Sci.* 274(2), 555-562. DOI: 10.1016/j.jcis.2003.12.029

Kissinger, H. E. (1957). "Reaction kinetics in differential thermal analysis," *Anal. Chem.* 29(11), 1702-1706. DOI: 10.1021/ac60131a045

Korb, J. (2007). "Termites," *Curr. Biol.* 17(1), 995-999. DOI: 10.1016/j.cub.2007.10.033

Laborie, M. P. G. (2002). *Investigation of the Wood/Phenol-Formaldehyde Adhesive Interphase Morphology*, Ph. D. dissertation, Virginia Polytechnic Institute and State University, Blacksburg, VA.

Lee, J. U., and Oh, Y. S. (2010). "Properties of particleboard produced with liquefaction-modified phenol-formaldehyde adhesive," *Turk. J Agric. For.* 34(4), 303-308.

Lee, W. J., Chang, K. C., and Tseng, I. M. (2012). "Properties of phenol-formaldehyde resins prepared from phenol-liquefied lignin," *J. Appl. Polym. Sci.* 124(6), 4782-4788.

Lee, S., Wu, Q., and Smith, W. R. (2004). "Formosan subterranean termite resistance of borate-modified strand board manufactured from southern wood species: A laboratory trial," *Wood fiber Sci.* 36(1), 107-118.

Lee, S. H., Yoshioka, M., and Shiraishi, N. (2000). "Preparation and properties of phenolated corn bran (CB)-phenol formaldehyde co-condensed resin," *J. Appl. Polym. Sci.* 7(13), 2901-2907. DOI: 10.1002/1097-4628(20000923)77:13<2901::AID-APP12>3.0.CO;2-F

Lei, Y., and Wu, Q. (2006). "Cure kinetics of aqueous phenol-formaldehyde resins used for oriented strand board manufacturing: Effect of wood flour," *J. Appl. Polym. Sci.* 102(4), 3774-3781. DOI: 10.1002/app.24739

Lin, J. Z., Chow, T. T., Fei, Y., Jianjun, Z., and Yanghui, Z. (2005). "A partial differential model for the pyrolysis of materials with movable residual layer," *Mech. Adv. Mater. Struc.* 12(2), 77-83. DOI: 10.1080/15376490490491990

Mendu, V., Harman-Ware, A. E., Crocker, M., Jae, J., Stork, J., Morton, S., Placido, A., Huber, G., and DeBolt, S. (2011). "Identification and thermochemical analysis of high-lignin feedstocks for biofuel and biochemical production," *Biotechnol. Biofuel.* 4(1), 1-14. DOI: 10.1186/1754-6834-4-43

Mendu, V., Shearin, T., Campbell, J. E., Stork, J., Jae, J., Crocker, M., Huber, G., and DeBolt, S. (2012). "Global bioenergy potential from high-lignin agricultural residue," *Proceedings of the NAS, USA* 109(10), 4014-4019. DOI: 10.1073/pnas.1112757109

Mohan, D., Shi, J., Nicholas, D. D., Pittman Jr, C. U., Steele, P. H., and Cooper, J. E. (2008). "Fungicidal values of bio-oils and their lignin-rich fractions obtained from

wood/bark fast pyrolysis," *Chemosphere*, 71(3), 456-465. DOI: 10.1016/j.chemosphere.2007.10.049

Mourant, D., Yang, D. Q., Lu, X., and Roy, C. (2005). "Anti-fungal properties of the pyroligneous liquors from the pyrolysis of softwood bark," *Wood fiber Sci.* 37(3), 542-548.

Mourant, D., Yang, D. Q., and Roy, C. (2007). "Decay resistance of PF-pyrolytic oil resin-treated wood," *Forest Prod. J.* 57(5), 30-35.

Nandika, D., Rismayadi, Y., and Diba, F. (2003). "Termites: Biology and its control," Muhammadiyah University Press, Solo, Indonesia.

Park, B. D., Riedl, B., Hsu, E. W., and Shields, J. (1998). "Effects of weight average molecular mass of phenol formaldehyde adhesives on medium density fiberboard performance," *Eur. J. Wood Wood Prod.* 56(3), 155-161. DOI: 10.1007/s001070050289

Park, B. D., Riedl, B., Hsu, E. W., and Shields, J. (1999). "Differential scanning calorimetry of phenol-formaldehyde resins cure-accelerated by carbonates," *Polymer* 40(7), 1689-1699. DOI: 10.1016/S0032-3861(98)00400-5

Rivilli, P. L., Alarcón, R., Isasmendi, G. L., and Pérez, J. D. (2011). "Stepwise isothermal fast pyrolysis (SIFP). Part II. SIFP of peanut shells – Antifungal properties of phenolic fractions," *BioResources* 7(1), 112-117.

Robison, R. G. (1972). *Wood-Coating Interactions*, Ph. D. dissertation, State University College of Forestry at Syracuse University, Syracuse, NY.

Sellers Jr, T. (1994). "Adhesives in the wood industry," *Handbook of Adhesive Technology*, 599-614.

Shahid, S. A., Ali, M., and Zafar, Z. I. (2014). "Characterization of phenol-formaldehyde resins modified with crude bio-oil prepared from *Ziziphus mauritiana* endocarps," *BioResources* 9(3), 5362-5384. DOI: 10.15376/biores.9.3.5362-5384

Shanbhag, R. R., and Sundararaj, R. (2013). "Physical and chemical properties of some imported woods and their degradation by termites," *J. Insect Sci.* 13(63), 1-8. DOI: 10.1673/031.013.6301

Stamm, A. J. (1964). *Wood and Cellulose Science*, Ronald Press, New York, 312-342.

Temiz, A., Alma, M. H., Terziev, N., Palanti, S., and Feci, E. (2010). "Efficiency of bio-oil against wood destroying organisms," *J. Biobased Mater. Bio.* 4(4), 317-323. DOI: 10.1166/jbmb.2010.1092

Temiz, A., Akbas, S., Panov, D., Terziev, N., Alma, M. H., Parlak, S., and Kose, G. (2013). "Chemical composition and efficiency of bio-oil obtained from giant cane (*Arundo donax* L.) as a wood preservative," *BioResources* 8(2), 2084-2098. DOI: 10.15376/biores.8.2.2084-2098

Turunen, M., Alvila, L., Pakkanen, T. T., and Rainio, J. (2003). "Modification of phenol-formaldehyde resol resins by lignin, starch and urea," *J. Appl. Polym. Sci.* 88(2), 582-588. DOI: 10.1002/app.11776

Vázquez, G., González-Álvarez, J., López-Suevos, F., Freire, S., and Antorrena, G. (2002). "Curing kinetics of Tannin-phenol-formaldehyde adhesives as determined by DSC," *J. Therm. Anal. Calorim.* 70(1), 19-28. DOI: 10.1023/A:1020680928311

Verma, M, Sharma, S, and Prasad, R. (2010). "Biological alternatives for termite control: A review," *Int. Biodeter. Biodegr.* 63(8), 959-972. DOI: 10.1016/j.ibiod.2009.05.009

Wahab, N. H. A., Tahir, P. M., Hoong, Y. B., Ashaari, Z., Yunus, N. Y. M., Uyup, M. K. A., and Shahri, M. H. (2012). "Adhesion characteristics of phenol formaldehyde pre-

preg oil palm stem veneers," *BioResources* 7(4), 4545-4562. DOI: 10.15376/biores.7.4.4545-4562

Wang, X. M., Riedl, B., Christiansen, A. W., and Geimer, R. L. (1995). "The effects of temperature and humidity on phenol-formaldehyde resin bonding," *Wood Sci. Technol.* 29(4), 253-266. DOI: 10.1007/BF00202085

Wang, M., Wei, L., and Zhao, T. (2005). "Cure study of addition-cure-type and condensation-addition-type phenolic resins," *Eur. Polym. J.* 41(5), 903-912. DOI: 10.1016/j.eurpolymj.2004.11.036

Wang, M., Leitch, M., and Xu, C. (2009a). "Synthesis of phenolic resol resins using cornstalk derived bio-oil produced by direct liquefaction in hot compressed phenol-water," *J. Ind. Eng. Chem.* 15(6), 870-875. DOI: 10.1016/j.jiec.2009.09.015

Wang, M., Xu, C., and Leitch, M. (2009b). "Liquefaction of cornstalk in hot-compressed phenol-water medium to phenolic feedstock for the synthesis of phenol-formaldehyde resin," *Biores. Technol.* 100(7), 2305-2307. DOI: 10.1016/j.biortech.2008.10.043

Wen, M. Y., Shi, J. Y., and Park, H. J. (2013). "Dynamic wettability and curing characteristics of liquefied bark-modified phenol formaldehyde resin (BPF) on rice straw surfaces," *J. Wood Sci.* 59(3), 262-268. DOI: 10.1007/s10086-013-1329-3

Zhang, W., Ma, Y., Xu, Y., Wang, C., and Chu, F. (2013). "Lignocellulosic ethanol residue-based lignin-phenol-formaldehyde resin adhesive," *Int. J. Adhes. Adhes.* 40(1), 11-18. DOI: 10.1016/j.ijadhadh.2012.08.004

Article submitted: August 25, 2014; Peer review completed: October 15, 2014; Revised version received and accepted: November 3, 2014; Published: November 11, 2014.